SOCAR Proceedings

Drilling & Completion

journal home page: http://proceedings.socar.az

A HYBRID BIONIC STRATEGY TO ENHANCE THE STATIC CHARACTERISTICS OF ROLLER-CONE BIT BEARINGS USING CFD SIMULATIONS

K. A. Bashmur*[1], A. V. Zagulyaev[1], M. V. Nebylitsyn[2]

[1]*Siberian Federal University, Krasnoyarsk, Russia*

[2]*Schneider Electric, Fairfield, OH, United States of America*

A B S T R A C T

The service life of roller-cone drill bits is largely determined by the condition of their bearing units, which account for a significant share of drilling failures. Reducing friction and increasing load-carrying capacity in bearing assemblies are essential for improving rock-breaking efficiency and extending tool life. One promising approach is the use of a bionic surface texture, which stabilizes the lubricant film and redistributes pressure within the contact zone. In this work, a combined bionic surface texturing strategy is proposed for the thrust bearing of a roller-cone bit, integrating a phyllotactic-inspired distribution pattern with ellipsoidal micro-dimples in both symmetric and asymmetric configurations. A CFD model of the thrust bearing was developed using numerical simulations in ANSYS Fluent. Smooth and textured surfaces were compared. Analysis of pressure distribution and shear stress demonstrated that the combined texture increases the load-carrying capacity of the lubricant film by up to 9% and the phyllotactic pattern reduces the friction coefficient by more than two times compared to a smooth surface. Additionally, a comparison between the phyllotactic pattern and a linear arrangement of micro-dimples showed a 14% reduction in friction coefficient with a slight decrease in load-carrying capacity. The obtained results confirm the effectiveness of the bionic approach in the design of roller-cone bit bearings and can be applied to develop wear-resistant and energy-efficient structures that contribute to increasing the maintenance interval of drilling tools.

Keywords: roller-cone bit; bearing; bionic surface texturing; phyllotactic; ellipsoidal dimples; CFD.

Date submitted: 24.11.2025 **Date accepted:** 09.02.2026

Introduction

With increasing depth and growing geological and technical complexity of drilling conditions, the requirements for reliability of drilling equipment and tools are rising. Roller-cone bits remain one of the key elements determining the efficiency of rock destruction, ensuring drilling process stability across a wide range of geological conditions. Their design combines rotational motion with cone rolling, enabling effective crushing and chipping of rock at moderate energy consumption. According to modern research [1–3], roller-cone bits still account for a significant portion of the total footage drilled in oil and gas wells, and bit longevity notably affects drilling economics. Compared to fixed cutter bits such as PDC, roller-cone bits perform better when drilling hard and tough formations, as well as during abrupt changes in formation lithology, providing a more stable drilling process in heterogeneous reservoirs [1, 2]. Due to their high versatility, repairability, and ability to operate under variable conditions, roller-cone bits remain relevant for developing various types of deposits, including deep and high-temperature horizons [1–3].

Despite the active development of drilling technologies and improvement in drilling tools, the durability of roller-cone bits remains a limiting factor for drilling process efficiency [1, 4, 5]. Under complex geological and technical conditions, the bit is the component of the bottom-hole assembly most frequently responsible for forced shutdowns and subsequent downtime due to costly tripping operations [1, 4, 5]. Analysis of operational data and failure results shows that up to 70–80 % of roller-cone bit failures are associated with damage to the bearing assembly [4–7]. The main causes of bearing failure include wear and fatigue damage of working surfaces, lubricant film degradation, seal failure, and uneven load distribution in the contact zone [4, 8–11]. Impact and vibration loads, as well as penetration of abrasive particles from drilling fluid, significantly accelerate damage development and reduce lubricant film stability [2, 12, 13].

Improvement of roller-cone bit bearing assemblies over recent decades has proceeded in several interrelated directions. Surface hardening and heat treatment methods for contact surfaces aimed at increasing hardness, fatigue strength, and wear resistance of bearing components have gained the widest application [6, 8, 14]. Significant contributions have been made by research on optimization of bearing materials

**E-mail:* kbashmur@sfu-kras.ru

http://dx.doi.org/10.5510/OGP20260201192

– from alloyed steels and copper alloys to specialized hardfacing and antifriction coatings with enhanced thermal conductivity and corrosion resistance [6, 8, 11, 14]. Alongside this, new design solutions have been developed: thread-locked bearings, floating bushings, combined bearings, as well as improved lubrication and sealing systems [3, 7, 13, 15, 16]. Nevertheless, even with such measures, zones of local overheating, uneven pressure distribution, and accelerated wear persist during prolonged operation under variable loads, limiting bearing life [5, 9–11].

In recent years, bionic approaches to improving wear resistance and energy efficiency of tribological systems have seen notable development, based on borrowing principles from nature-inspired structures and rational organization of surface microtexture [17–22]. Within this framework, formation of specialized microtexture on bearing working surfaces is considered a particular case of bionic design: regularly organized grooves and micro-dimples promote lubricant retention, pressure redistribution, and formation of local hydrodynamic support zones, reducing friction and stabilizing the lubricant film [9, 10, 23, 24]. The use of such textured surfaces has demonstrated high effectiveness in creating components of hydromechanical systems and can be adapted to roller-cone bit bearing assemblies operating under mixed friction and boundary lubrication conditions [3, 4, 13, 20]. Within the «green tribology» concept, improving bearing and bit characteristics is also viewed as a tool for reducing energy consumption and environmental impact of mining and oil-and-gas equipment [17, 20–22].

Experimental studies by Lu et al. [23, 24] showed that applying the phyllotactic principle for dimple placement – consisting of quasi-regular spiral arrangement of micro-dimple centers with an angular step close to the «golden» angle – provides more uniform lubricant distribution and reduces the friction coefficient by 15–30 % compared to regular grid patterns. Zhong et al. [9] established that using elliptical micro-dimples on roller-cone bit bearings increases bearing load capacity and reduces wear intensity. In related oil and gas industry applications, similar microscale structures, as well as wettability control and flow redistribution methods, are used for evaluating the thermomechanical state of rock framework, conducting water shutoff treatments, and improving enhanced oil recovery systems [25–29]. However, we are not aware of studies combining the phyllotactic pattern with ellipsoidal micro-dimple geometry for bit bearings. Additionally, the hypothesis proposed by Yu et al. [30, 31] regarding the use of asymmetric ellipsoids to influence the hydrodynamic wedge effect and narrow the cavitation zone in the dimple was investigated. However, the effect of ellipsoidal micro-dimples with shifted apex on the static characteristics of thrust bearings under the specific operating conditions of bit bearings has not been previously considered. All this formed the basis for the present study of the combined effect of using bionic microtexture, its special organization, and adaptation to roller-cone bit bearing operating conditions: a combined bionic strategy is considered, integrating the phyllotactic dimple placement pattern and special micro-dimple shapes.

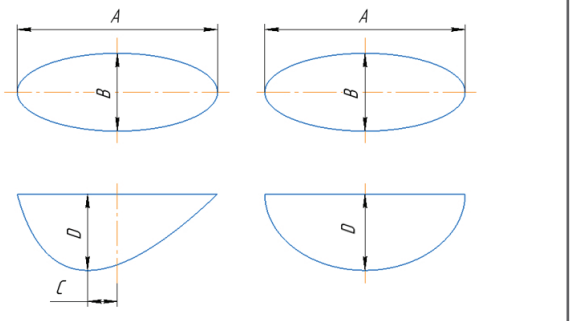

Fig. 1. Schematic representation of surface texture microdimples

The aim of this work was to investigate the technological capabilities of combined bionic surface texture for roller-cone bit bearings based on a thin-film computational fluid dynamics numerical model. Research objectives included: analysis of existing methods for improving wear resistance and load capacity of roller-cone bit bearing assemblies; development of a hybrid bionic surface microtexture strategy; comparative modeling of smooth and textured surfaces; and evaluation of the effect of texture geometric parameters on bearing static characteristics.

Methods

The object of the study was a thrust bearing of a roller-cone bit, modeled as a segment of the contact pair «bearing disk – cone» with a thin lubricant film. The subject of the study was a special bionic texture of the bushing working surface, combining special surface microtexture with its arrangement in a phyllotactic pattern. This approach allows the transfer of organizational principles from nature-inspired surfaces into engineering practice. In particular, the elytra of diving beetles of the *Dytiscidae* family exhibit ellipsoidal microtextures that ensure moisture retention and film stability under high loads [32, 33], while the phyllotactic distribution of dimples – analogous to the spiral arrangement of sunflower seeds or pine cone scales – provides uniform surface coverage without overlaps or voids [34].

In modeling the ellipsoidal microtexture, two geometry variants were considered – coaxial and with axial apex offset of the dimples, which allowed evaluating the effect of structural asymmetry on pressure distribution and development of microflows in the lubricant layer. Each dimple was described by an ellipsoid with semi-axes A and B, and depth D. The offset variant was characterized by parameter C, defining the deviation of the ellipsoid apex from the center. Figure 1 presents a schematic representation of microdimples for cases with and without ellipsoid apex offset.

Thus, four configurations of the thrust bearing working surface were used:

1. smooth surface;
2. surface with linearly arranged texture, i.e., an array of concentric circles with linear spacing containing ellipsoidal dimples;
3. surface with texture arranged in a phyllotactic pattern containing ellipsoidal dimples (without apex offset, i.e., the depth profile is symmetric);
4. surface with texture arranged in a phyllotactic pattern containing ellipsoidal dimples (with apex offset, i.e., the depth profile is asymmetric), which may allow pressure redistribution in the working zone, reduce the probability of cavitation and its effects.

The first two configurations were used for comparison

with the phyllotactic pattern to determine the achieved effect. For adequate assessment of the friction coefficient, all textured configurations used the same area, referred to as the relative bearing surface area.

At the next stage, a geometric model of the bearing surface with bionic texture was developed. A section of the thrust bearing was used as the basis, on the inner surface of which ellipsoidal dimples were specified, arranged either linearly along concentric circles (fig. 2a) or according to the phyllotactic distribution law (fig. 2b), implemented using Vogel's model for a flat surface [35]. The following relationships were used to specify the coordinates of dimple centers:

$$\varphi_n = n\theta, \quad \rho_n = c\sqrt{n} \tag{1}$$

where $n=0,1,2,\ldots$, $n_{\max}$ – sequential number of the dimple, φ_n – angular coordinate; ρ_n – distance from the center; $\theta=\pi(3-\sqrt{5})\approx137.5°$ – golden angle; $c=0.6$ – coefficient determining the distance between adjacent dimple centers, chosen based on equality of areas occupied by the texture in different configurations to exclude the influence of this factor on the friction coefficient. This arrangement allows forming a uniform quasi-regular distribution of dimples without axial symmetries and clustering zones, analogous to the spiral structure of sunflower seeds or conifer scales.

Figure 3 presents a textured roller-cone bit bearing with phyllotactic pattern and the location of the modeled thrust bearing within it: a) the arrow indicates the contact pair zone «bearing disk – cone»; b) shows a sector of the thrust bearing with main geometric dimensions.

The initial geometric parameters of the surface texture, operating conditions, and lubricant properties used in the calculations are given in table 1.

Regarding the selection of ellipsoidal micro-dimple parameters, we used data from work [36], in which optimal characteristics of a thrust bearing with micro-dimples having an offset ellipsoid axis were investigated based on the Grey-Taguchi Method. Parametric analysis of parameter influence or other optimization procedures were not conducted in the present work and constitute a topic for separate research.

Figure 4 shows the modeled thrust bearing segment with linear texture arrangement and dimensions.

Computational fluid dynamics methods based on the ANSYS Fluent software package were used in this work. Considering the specifics of bit bearing lubrication, the ANSYS Fluent module with the viscous model «Laminar» (Models → Viscous → Laminar) was used. In this formulation, the Navier-Stokes equations are solved without turbulent closure; additional transport equations (k-ε, k-ω, etc.) are not introduced. The energy equation was disabled, temperature effects were not considered, and lubricant properties were specified as constant.

The Navier-Stokes equation system for incompressible fluid [37]

$$\begin{cases} \nabla \cdot v = 0, \\ \rho (v \cdot \nabla) v = -\nabla p + \mu \nabla^2 v, \end{cases} \tag{2}$$

where ρ – lubricant layer density; μ – dynamic viscosity of the lubricant layer; v – velocity of lubricant layer flow; p – lubricant layer pressure. For all surface configurations, static pressure fields $p(x,y)$ and shear velocities near the wall u_t were extracted from calculations. The following were then computed:

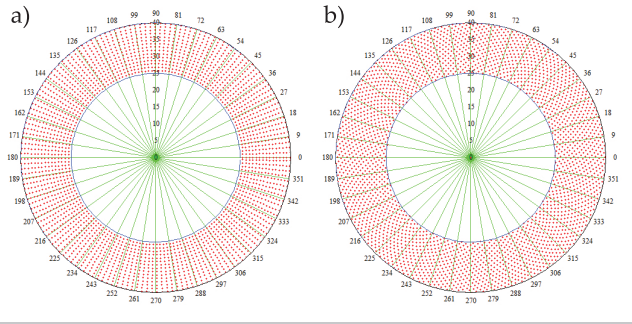

Fig. 2. Microdimple arrangement: a) linear; b) with phyllotactic pattern

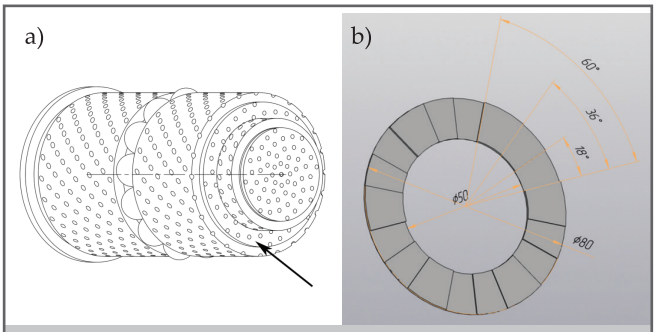

Fig. 3. Roller cone bit bearing with texture (a) and the research object – thrust bearing (b)

Table 1

Input parameters for modeling

Parameter name	Value
Lubricant density	876 kg/m³
Dynamic viscosity of lubricant	0.0125 Pa·s
Minimum oil film thickness	25 μm
Lubricant supply pressure	0.2 MPa
Lubricant supply method	from inner side
Cone rotational speed	100 rpm
Ambient temperature	50 °C
Ellipsoid major axis length	550 μm
Ellipsoid minor axis length	280 μm
Ellipsoid apex offset magnitude	180 μm
Ellipsoid depth	60 μm

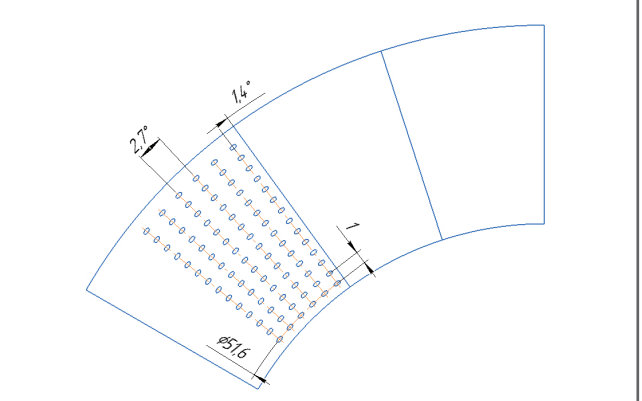

Fig. 4. Dimple arrangement on the surface of the thrust bearing segment

1. Area-weighted average pressure of the lubricant layer

$$\overline{p}_A = \frac{1}{A}\iint_S p\,\mathrm{d}A \tag{3}$$

where A – modeling surface area.

2. Load-carrying capacity of the lubricant layer

$$W_S = \iint_S p\,\mathrm{d}A \tag{4}$$

3. Wall shear stress for the laminar model

$$\tau_w = \mu \left.\frac{\partial u_t}{\partial n}\right|_{wall} \tag{5}$$

where n – unit normal to the wall.

4. Local friction coefficient of the lubricant layer and its area averaging

$$C_f = \frac{\tau_w}{1/2\rho U_{\mathrm{ref}}^2}, \quad \langle C_f \rangle_A = \frac{1}{A}\iint_S C_f\,\mathrm{d}A, \tag{6}$$

where U_{ref} – reference velocity.

5. Friction force of the lubricant layer and friction coefficient

$$F_\tau = \iint_S \tau_w\,\mathrm{d}A, \quad \mu = F_\tau / W_S \tag{7}$$

The computational domain represented a thin lubricant layer of the contact pair «bearing disk – cone» within the working arc of the bearing (figs. 4 and 5). The lateral boundaries of the sector were assumed to be symmetry/periodicity planes.

Flow was specified on the radial planes of the thrust bearing sector. At the inlet plane, the velocity was set to 1.73 m/s, and at the opposite plane, the gauge pressure was set to 0.2 MPa. The inner and outer arcs were treated as solid walls. The lower wall was considered to be moving with a rotational speed of 100 rpm, while the upper wall remained stationary. The boundary condition scheme is shown in figure 6.

Next, discretization of the computational domain was performed using a three-dimensional unstructured tetrahedral finite element mesh. The mesh independence test is presented in table 2.

Thus, for the smooth surface, a uniform mesh was used (fig. 7), containing 19080 elements.

For surfaces with bionic texture, additional mesh refinement was performed in the zone of ellipsoidal dimples while maintaining a moderate total number of elements. Figure 8 shows the general view of the mesh and its enlarged fragment for the thrust bearing with linear dimple arrangement. The total number of elements for the bearing with special pattern was 2331946 for the configuration without offset and 1939416 for the configuration with apex offset. For the linear configuration – 2074876 elements. As a result of increasing the computational mesh detail caused by the complexity of the model geometry, a significant increase in the total number of elements occurred. At the same time, in all cases the sector geometry, boundary conditions, and physical model remained identical.

To solve the Navier-Stokes equations (2), it is necessary to compute the pressure field, since pressure gradients arise in the momentum equations. Pressure-velocity coupling

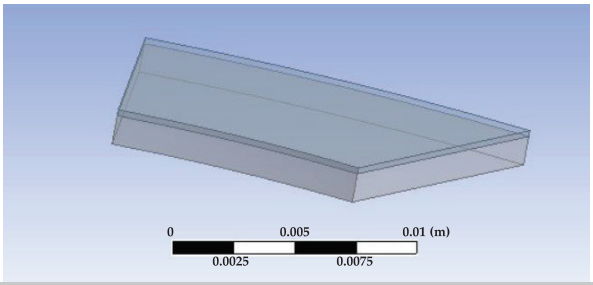

Fig. 5. Geometry of the bit support thrust bearing

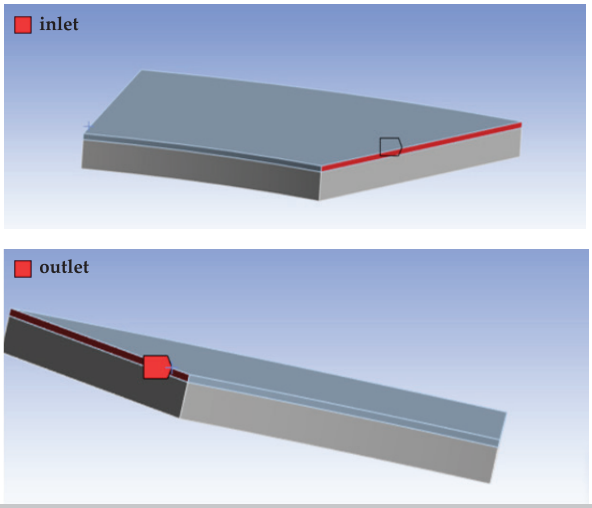

Fig. 6. Boundary conditions scheme

Table 2

Mesh independence study

Mesh Density	Maximum Static Pressure, MPa
Smooth Surface	
14978	0.223
19080	0.230
54894	0.229
125574	0.230
Phyllotactic and Dimples (no offset)	
1318242	0.232
1489658	0.251
1943842	0.263
2331946	0.266
3145320	0.267

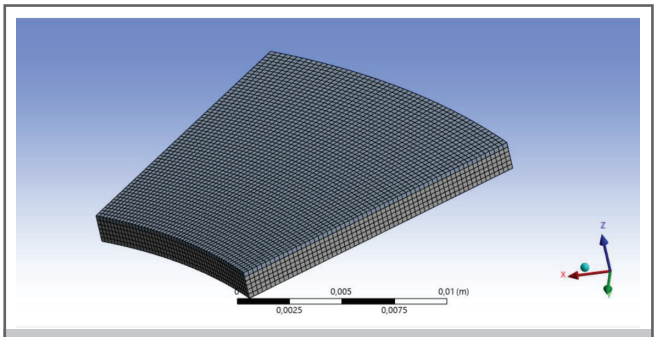

Fig. 7. Computational mesh for smooth surface

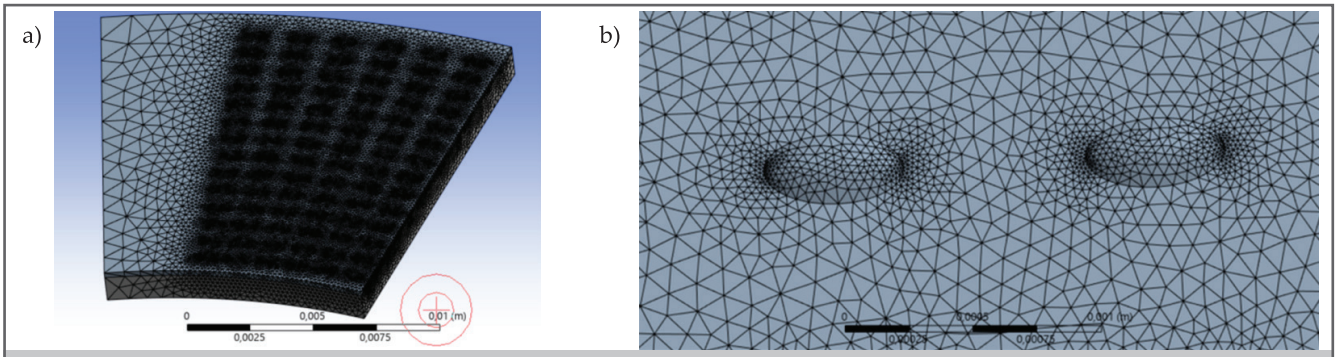

Fig. 8. Computational mesh of the textured bearing: a) general view; b) enlarged fragment in the texture zone

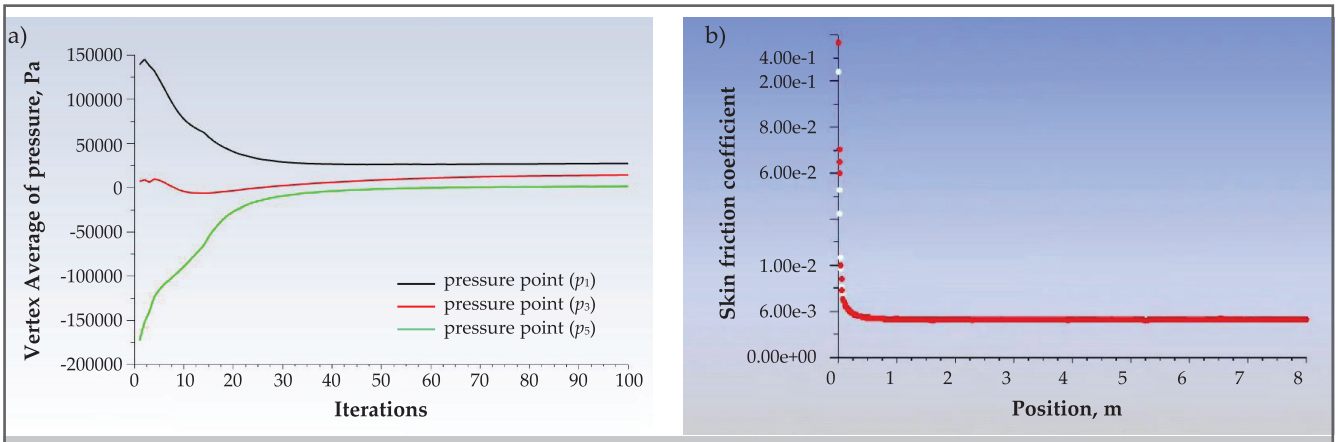

Fig. 9. Convergence plot of the main investigated bearing parameters: a) static pressure; b) and friction coefficient

algorithms (schemes) are used to obtain pressure from the momentum and continuity equations. The following algorithms used in ANSYS Fluent were compared based on the number of iterations and time spent: SIMPLE, SIMPLEC, COUPLED. Convergence of the COUPLED method proved difficult to achieve, probably due to the laminar flow of lubricant in the bearing. The first two methods converged with the same value of the target parameter – static pressure. However, for SIMPLE, convergence occurred faster and with fewer iterations. Thus, the SIMPLE algorithm proved to be the most suitable algorithm with the fastest convergence. For each calculation, the number of iterations (calculation steps) was set to 100. The process was considered steady-state within the specified number of iterations when the values of static pressure and friction coefficient reached a certain constant value. The convergence plot («residuals») of the main investigated parameters is presented in figure 9. In particular, to assess the reliability of pressure calculation, we set three points directly at the center (p_3), as well as before (p_5) and after the center (p_1) on the surface of the ellipsoidal dimple and specified local «Vertex Average» monitors to track average pressure values at these points, as shown in the pressure profile of the ellipsoidal microdimple in figure 10. Also, figure 9b presents the friction coefficient convergence plot for the smooth surface.

Thus, the solution reached steady state within 100 iteration steps. The pressure differential (fig. 9) indicates the presence of convergence/divergence angles of the hydrodynamic wedge, as does the pressure profile in figure 10. The friction coefficient after the break-in period (start of operation after startup) assumes a constant value of 0.006, indicating a hydrodynamic friction regime in the thrust sliding bearing.

The reliability of the numerical model was verified against the experiment for a thrust bearing with phyllotactic texture from work [24]. The following parameters from the graph ([24], fig. 13) were selected as reference points: axial force F=950 N, dimple diameter d=2 mm, phyllotactic coefficient c=2 and variable rotational speed. At n=235 rpm, the graph yields a friction coefficient of approximately 0.005. In a comparable numerical calculation for these conditions, we obtained a friction coefficient of 0.0047. The relative discrepancy was 6%. Possible causes of discrepancy include: heating of the assembly during testing and viscosity drop of the L-AN46 oil used, differences between the rheological properties of the lubricant and those assumed in the model, weak inertial/quasi-turbulent effects, as well as texture geometry tolerances. This value is considered acceptable and confirms the validation of the model based on the key integral parameter.

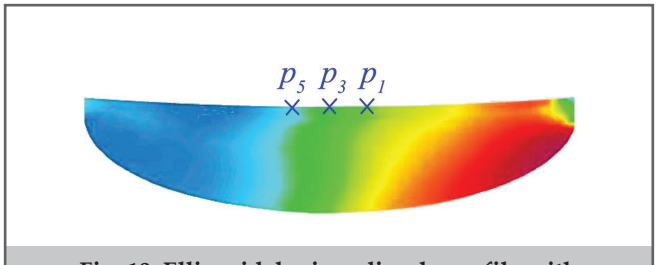

Fig. 10. Ellipsoidal micro-dimple profile with «Vertex Average» monitor installation locations

Results and discussion

During the numerical modeling of the thrust bearing, static pressure distributions were obtained and friction coefficients were calculated for four variants of working surface geometry. These parameters allow evaluating the influence of microtexture on lubricant layer formation and bearing operation efficiency under hydrodynamic regime conditions.

Figure 11 presents the obtained area-weighted static pressure values, and figure 12 shows example static pressure distribution fields across the thrust bearing segment for the smooth surface and textured surface with phyllotactic pattern without ellipsoid axis offset.

The static pressure distributions shown in figures 11 and 12 demonstrate an overall pressure increase in the presence of texture. On the smooth surface (fig. 12a), the pressure is distributed relatively uniformly with a maximum in the central zone. In the case of the textured surface (fig. 12b), the formation of a more pronounced hydrodynamic wedge and an increase in local pressure in the direction of lubricant flow movement are observed. At the same time, the difference between textures with and without apex offset is insignificant, indicating a weak influence of dimple asymmetry on the pressure field formation.

The area-weighted static pressure values were: 0.210 MPa for the smooth surface; for the phyllotactic pattern without ellipsoid apex offset – 0.229 MPa, with ellipsoid apex offset – 0.226 MPa; for linear arrangement of ellipsoidal texture – 0.234 MPa. Thus, compared to the smooth surface, the presence of ellipsoidal texture provides a pressure increase of 7–9 % with the special surface pattern and 11.5% with linear texture arrangement. This result is attributed to the hydrodynamic wedge formation effect in ellipsoidal texture, whereby, due to the lubricant flow around the micro-dimple geometry, the initial pressure decrease is less than the subsequent pressure increase (blue zone of pressure distribution versus the rest in fig. 10). Apex offset leads to practically identical pressure increase results, and first-order effects should probably not be expected due to laminar lubricant flow and weakly developed cavitation. The advantages of ellipsoidal micro-dimples with apex offset were previously obtained for rotational speeds of 6000 rpm and developed turbulent lubricant flow regime [30, 36].

The sequential linear arrangement of micro-dimples along concentric circles (fig. 8) more clearly promotes accumulation of the hydrodynamic wedge effect along the lubricant layer movement, showing some advantage over the phyllotactic pattern, since according to (1), each subsequent dimple moves away from the center. This may be somewhat mitigated under real operating conditions with non-ideal lubricant flow; nevertheless, from the standpoint of increasing load-carrying capacity, linear arrangement evidently slightly exceeds the special pattern. The overall pressure increase indicates formation of a denser oil film capable of withstanding greater axial load without compromising lubricant layer integrity.

Figure 13 shows the velocity field for the textured surface.

The velocity vector field (fig. 13) confirms the ordered nature of the flow. The lubricant flow smoothly bypasses the dimples without forming stagnant zones or vortex structures, indicating stable flow and uniform pressure distribution across the surface.

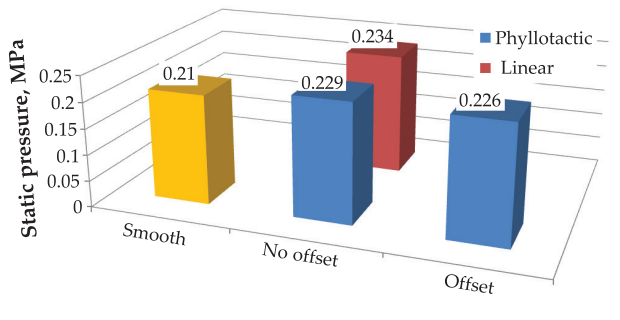

Fig. 11. Area-weighted static pressure values

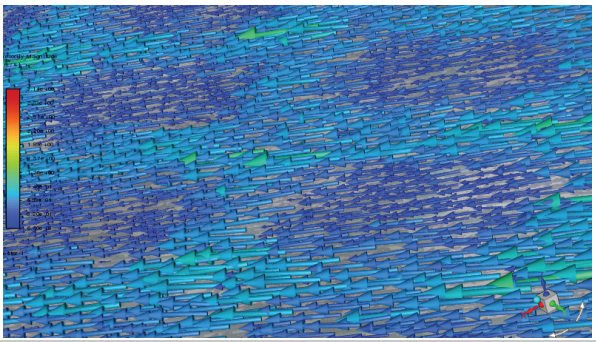

Fig. 13. Velocity field distribution in the bearing with texture

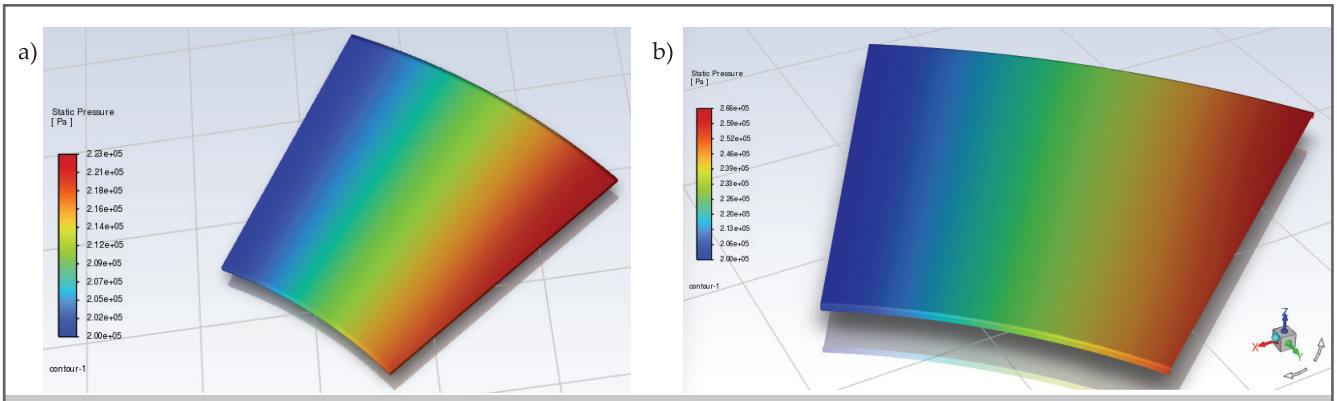

Fig. 12. Pressure field distribution for: a) smooth surface; b) textured surface without ellipsoid apex offset

Following the pressure distribution analysis, integral friction coefficients were evaluated for four surface geometry variants. A summary comparison of friction coefficients for the four configurations is presented in figure 14 as a bar chart. For quantitative assessment of shear stresses and integral friction losses, an ANSYS Fluent report was generated for the Skin Friction Coefficient parameter. As an example, Figure 15 shows values for the smooth surface and textured surface with phyllotactic pattern without ellipsoid axis offset. The report provides values corresponding to the contribution of the bearing wall «wall-podshipnik», the boundary with lubricant «wall-smazka», as well as the total indicator «Net», which was subsequently used for calculating the reduced friction coefficients.

It can be seen that the presence of texture reduces the friction coefficient by more than half, while the difference between phyllotactic texture variants with and without offset is minimal and statistically insignificant, which was an expected result and is not an anomaly. Thus, based on experimental studies of thrust bearings, Etsion et al. [38] obtained friction coefficient values for bearings with smooth surfaces 2.5–3 times higher than the corresponding values for bearings with spherical dimples at 1500 rpm, which was attributed to much smaller clearances in non-textured bearings and, consequently, higher shear stress. In a similar study with cylindrical dimples and their various arrangements, the authors [24] obtained a twofold reduction in friction coefficient with phyllotactic pattern versus linear arrangement, with the maximum difference observed under flow conditions close to laminar. According to modern understanding [39], confirmed in the present work, non-smooth surfaces help retain lubricant, which promotes formation of a stable oil film, increasing its load-carrying capacity and preventing dry friction caused by film rupture. Reduction of contact surface area in the tribological pair reduces intermolecular forces and thus minimizes adhesion. Also, as already noted, the presence of texture reduces lubricant shear stress when additional lubricant layers are present, which is especially important for the laminar lubricant flow regime.

Different micro-dimple arrangement variants lead to different oil film pressure distributions and lubricant flow rates formed on the bearing working surface. Thus, the friction coefficient for linear texture arrangement was 14% higher than the coefficient obtained for the special pattern, with equal areas occupied by the texture. Probably, the main factor here is the more uniform pressure distribution and, correspondingly, lubricant distribution across the thrust bearing working surface with phyllotactic microdimple filling (see fig. 2), which primarily affects oil film stability and lubrication regime. To some extent, this can be mitigated by increasing micro-dimple packing density in linear arrangement, which, however, may entail additional costs and difficulties in manufacturing such texture, including increased shape inaccuracies and roughness, as well as significant disruption of the pressure profile in the gap due to increased number of peaks and troughs on the pressure curve and, correspondingly, load-carrying capacity, and will probably negatively affect the dynamic characteristics of the bearing.

The final modeling results for all thrust bearing segment surface configurations, including area-weighted pressure, load-carrying capacity, and friction coefficient, are summarized in table 3.

Collectively, the presented pressure and velocity fields and integral metrics demonstrate a unified trend: regular ellipsoidal microtexture forms a more stable hydrodynamic regime with increased load-carrying capacity and reduced shear stresses compared to the smooth surface. The difference between «no offset» and «with offset» configurations is small, indicating the dominant role of the textured surface itself at similar geometric parameters of the dimples. The obtained results are consistent between local fields and integral estimates and provide the basis for subsequent optimization of texture parameters and consideration of thermoviscous and dynamic effects in further calculation series.

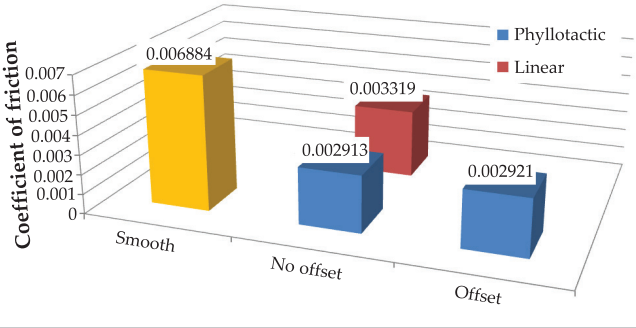

Fig. 14. Friction coefficient values

```
  Skin Friction Coefficient
---------------------------- --------------------
                wall-podshipnik                    0
                    wall-smazka            332.97268
---------------------------- --------------------
                            Net            145.20058

  Skin Friction Coefficient
---------------------------- --------------------
                wall-podshipnik                    0
                    wall-smazka            787.32555
---------------------------- --------------------
                            Net              343.3302
```

Fig. 15. Skin Friction Coefficient indicators for smooth and phyllotactic surface without offset

Table 3

Modeling results

Surface	Static pressure, MPa	Load capacity, N	Coefficient of friction
Smooth surface	0.210	128.58	0.006884
Phyllotactic dimples – no offset	0.229	140.22	0.002913
Phyllotactic dimples – offset	0.226	138.38	0.002921
Linear – no offset	0.234	143.28	0.003319

Conclusions

This work investigated a combined bionic strategy integrating a specialized micro-dimple placement pattern and their various shapes. Specifically, using the ANSYS Fluent software environment, numerical modeling was performed for a thrust bearing of a roller-cone bit with various working surface geometries: smooth, with discrete micro-dimples without ellipsoid apex offset, and with apex offset. Two variants of dimple arrangement on the bearing working surface were considered – phyllotactic pattern and linear arrangement. The influence of the microtexture on pressure distribution, load-carrying capacity, and friction coefficient under hydrodynamic lubrication conditions was evaluated. Summarizing the main results of the conducted research, the following conclusions can be drawn:

1. Based on the modeling results, it was established that the use of texture leads to an increase in area-weighted pressure and bearing load-carrying capacity. For the phyllotactic texture arrangement without offset, the static pressure value was 0.229 MPa, which is 9% higher than that of the smooth surface. With ellipsoid axis offset, the pressure decreases somewhat but remains above the baseline level of the smooth surface. The linear texture arrangement exceeds the phyllotactic pattern by 2.5% and under certain conditions, for example, in heterogeneous, layered, and interbedded formations, may be preferred due to expected intense tool vibrations.
2. Analysis of velocity distribution fields confirmed the stable laminar nature of lubricant flow without pronounced stagnant zones, indicating stability of the hydrodynamic regime at the selected texture parameters.
3. The friction coefficient in the presence of microtexture with phyllotactic arrangement decreases by more than half – from 0.006884 for the smooth surface to 0.002921 and 0.002913 for textures with and without offset, respectively. This is associated with pressure redistribution and formation of a more stable lubricant film that reduces shear stresses. The difference between the two phyllotactic texture variants is minimal and statistically insignificant. The presence of substantial gaps between dimples in radial and circumferential directions led to a 14% increase in friction coefficient for the linear arrangement compared to the phyllotactic pattern at equal areas occupied by the texture. Thus, phyllotactic arrangement of microtexture on the thrust bearing working surface leads to reduced torque losses at the bit and increased wear resistance of its bearing.
4. The obtained results confirm the effectiveness of a combined bionic strategy using ellipsoidal microtexture with phyllotactic arrangement for improving energy efficiency and service life of roller-cone bit bearing assemblies. The textured surface allows simultaneous increase in load-carrying capacity and reduction in friction losses without significant changes to the assembly design and operating principle. At the same time, the hypothesis of improving bit bearing characteristics through vertex offset of ellipsoidal dimples did not yield significant results, presumably due to poorly developed cavitation and insignificance of turbulent phenomena, and therefore is not of great interest for practical application in roller-cone bits. Moreover, this approach may require development of new manufacturing technologies for ellipsoidal structures with anisotropy to replace those known for non-offset textures via laser texturing [40], mechanical [41], and vibromechanical [42] surface treatment, utilization of complex technological operations and processes, including lathe tool motion with time delay or photonics methods for creating asymmetric laser beams, which may lead to deterioration of the formed surface topography quality due to non-uniformity of laser power fluctuations, expansion of cutting process control parameters, and other factors.
5. Computational fluid dynamics software allowed obtaining bearing characteristics with complex geometry with acceptable accuracy, significant time savings and other research resources, which is expected to be useful for researchers and designers of roller-cone bits, as well as other equipment where sliding bearings are used. Future work is planned in the direction of expanding parametric series for depth, shape, and spacing of dimples, as well as including thermoviscous effects and dynamic stability of the bit rotor-bearing system in the model. Such studies will enable optimization of texture geometry for specific operating conditions and bringing the results closer to practical application.

References

1. Abbas, R. K. (2018). A review on the wear of oil drill bits (conventional and the state of the art approaches for wear reduction and quantification). *Engineering Failure Analysis*, 90, 554–584.

2. Dai, X., Chen, P., Huang, T. (2024). Investigation on the rock failure characteristics and reliability of hybrid drill bits combing shaped PDC cutters and roller-cone elements. *Geoenergy Science and Engineering*, 239, 212976.

3. Moiseev, K. V., Popenov, A. I., Bakhtizin, R. N. (2021). Express method for the testing of tribotechnical properties of lubricants. *SOCAR Proceedings*, SI2, 65–69.

4. Huang, Z., Li, G. (2018). Failure analysis of roller cone bit bearing based on mechanics and microstructure. *Journal of Failure Analysis and Prevention*, 18, 342–349.

5. Shigin, A. O., Boreyko, D. A., Tskhadaya, N. D., Serikov, D. Yu. (2021). Comparative analysis of roller drill bit performance. *SOCAR Proceedings*, SI2, 001–007.

6. Liu, Ya., She, Ya., Li, W. (2025). Research on working mechanism and structural optimization of high-speed bearing of tricone bits based on finite difference method. *Journal of Tribology*, 147(4), 044103.

7. Valiev, N. G., Simisinov, D. I., Afanasiev, A. I. (2021). Loading tests of retaining tricone bit bearing using physical model. *Eurasian Mining*, 2, 60–64.

8. Huang, Z., Li, Q., Zhou, Y., et al. (2013). Experimental research on the surface strengthening technology of roller cone bit bearing based on the failure analysis. *Engineering Failure Analysis*, 29, 12–26.

9. Zhong, L., Wei, G., Wang, G., et al. (2020). Tribological properties of rock bit journal bearings for journal with nanosecond laser surface texture. *Tribology Transactions*, 63(6), 1020–1040.

10. Wang, G. R., Zhong, L., He, X., et al. (2014). Experimental study of tribological properties of surface texture on rock bit sliding bearings. *Proceedings of the Institution of Mechanical Engineers, Part J: Journal of Engineering Tribology*, 228(12), 1392–1402.

11. He, W., Chen, Y., He, J., et al. (2016). Spherical contact mechanical analysis of roller cone drill bits journal bearing. *Petroleum*, 2(2), 208–214.

12. Petrovsky, E. A., Bashmur, K. A., Shadchina, Yu. N., et al. (2024). Study of microrelief forming technology on sliding bearings for oil and gas centrifugal units. *Journal of Physics: Conference Series*, 1399(5), 055032.

13. Ismakov, R. A., Konesev, V. G., Yangirov, F. N., et al. (2021). Research of the kinetics of thickness of the boundary layers of lubricating materials applied to drilling technology. *SOCAR Proceedings*, 2, 115–120.

14. Šporin, J., Mrvar, P., Janc, B., Vukelić, Ž. (2021). Expression of the self-sharpening mechanism of a roller cone bit during wear due to the influence of the erosion protection carbide coating. *Coatings*, 11, 1308.

15. Zhou, Y., Wang, R., Hu, J., Lei, X. (2023). High-temperature wear mechanism of roller cone bit spiral seal. *Wear*, 532–533, 205112.

16. Simisinov, D. I., Afanas'ev, A. I., Valiev, N. G. (2021). Reducing the load on the roller bit support. *Mining Informational and Analytical Bulletin*, 11-1, 197–208.

17. Li, W., Li, Y., Fan, J., et al. (2025). Experimental study on the tribological performance of shark denticle-inspired texture for roller cone bit bearings. *Lubricants*, 13, 468.

18. Atwal, J. C., Pandey, R. K. (2021). Performance analysis of thrust pad bearing using micro-rectangular pocket and bionic texture. *Proceedings of the Institution of Mechanical Engineers, Part J: Journal of Engineering Tribology*, 235(6), 1232–1250.

19. Kumar, R., Rezapourian, M., Rahmani, R., et al. (2024). Bioinspired and multifunctional tribological materials for sliding, erosive, machining, and energy-absorbing conditions: a review. *Biomimetics*, 9, 209.

20. Cohen, I., Goltsberg, R. (2023). Partial surface texturing in hydrodynamic lubrication: a CFD-based investigation. *Lubricants*, 11(9), 395.

21. Bashmur, K. A., Zagulyaev, A. V., Agafonov, E. D., Nebylitsyn, M. V. (2025). Green tribology concepts: a potential for sustainable development of themining machinery with sliding bearings. Sustainable *Development of Mountain Territories*, 2(17), 787–797.

22. Kukartsev, V. A., Kukartsev, V. V., Tynchenko, V. S., et al. (2022). The technology of using liquid glass mixture waste for reducing the harmful environmental impact. *Materials*, 15(3), 1220.

23. Lu, Y., Liu, Y., Wang, J., Liu, H. (2014). Experimental investigation into friction performance of dimples journal bearing with phyllotactic pattern. *Tribology Letters*, 55, 271–278.

24. Lu, Y., Liu, Y., Wang, J., Liu, H. (2016). Tribological performance of dimpled thrust bearings with phyllotactic patterns. *Wear*, 346–347, 108–115.

25. Suleimanov, B. A., Feyzullayev, K. A. (2024). Simulation study of water shut-off treatment for heterogeneous layered oil reservoirs. *Journal of Dispersion Science and Technology*, 46(10), 1594–1604.

26. Tan, J., Melkoumian, N., Harvey, D., Akmeliawati, R. (2025). Nature-inspired solutions for sustainable mining: applications of NIAs, swarm robotics, and other biomimicry-based technologies. *Biomimetics*, 10, 181.

27. Suleimanov, B. A., Abbasov, H. K. (2024). Wettability alteration of quartz sand using Z-type Langmuir–Blodgett hydrophobic films. *Physics of Fluids*, 36(3), 034118.

28. Tynchenko, V., Kurashkin, S., Tynchenko, V., et al. (2021). Mathematical modeling of induction heating of waveguide path assemblies during induction soldering. *Metals*, 11(5), 697.

29. Suleimanov, B. A., Rzayeva, S. J., Akhmedova, U. T. (2021). Self-gasified biosystems for enhanced oil recovery. *International Journal of Modern Physics B*, 35(27), 2150274.

30. Yu, Y., Zhou, L., Ruan, W., et al. (2023). Characteristic analysis and optimization of sliding bearings with special-shaped microtextured multi-oil wedges. *Journal of Northwestern Polytechnical University*, 41(1), 222–229.

31. Xu, P., Luo, J., Yu, Y., et al. (2025). Comprehensive performance and optimization of micro textured slipper pair of axial piston pumps. *Scientific Reports*, 15, 12508.

32. Cheng, H., Ce, G., Tao, X. (2018). Bionic design inspired by surface texture of Cybister's Elytra. *Transactions of Nanjing University of Aeronautics and Astronautics*, 35(S), 51–58.

33. Yang, Z., Dai, Z., Guo, C. (2010). Morphology and mechanical properties of Cybister elytra. *Chinese Science Bulletin*, 55, 771–776.

34. Barthlott, W., Neinhuis, C. (1997). Purity of the sacred lotus, or escape from contamination in biological surfaces. *Planta*, 202, 1–8.

35. Vogel, H. (1979). A better way to construct the sunflower head. *Mathematical Biosciences*, 44(3–4), 179–189.

36. Li, J. (2022). Multi-objective optimization design and performance analysis of micro-texture of thrust plain bearing. *Master's Theses. Liaoning Technical University*.

37. Matsson, J. E. (2024). An introduction to Ansys Fluent 2024. *USA: SDC Publications.*

38. Etsion, I., Halperin, G., Brizmer, V., Kligerman, Y. (2004). Experimental investigation of laser surface textured parallel thrust bearings. *Tribology Letters*, 17(2), 295–300.

39. Sasaki, S. (2024). Surface texturing for friction control: A review on existing technology and prospects. *Tribology Online*, 19(2), 105–120.

40. Paul Joshua, S., Dinesh Babu, P. (2020). Effect of laser textured surface with different patterns on tribological characteristics of bearing material AISI 52100. *Journal of Central South University*, 27, 2210–2219.

41. Bashmur, K. A., Petrovsky, E. A. (2023). Equipment for creating cellular relief on frictional surfaces. *Russian Engineering Research*, 43, 983–986.

42. Kurniawan, R., Kiswanto, G., Ko, T. J. (2017). Surface roughness of two-frequency elliptical vibration texturing (TFEVT) method for micro-dimple pattern process. *International Journal of Machine Tools and Manufacture*, 116, 77–95.